Supplement of Clim. Past, 18, 249–271, 2022
https://doi.org/10.5194/cp-18-249-2022-supplement

Climate of the Past
Open Access
EGU

Supplement of

Abrupt climate changes and the astronomical theory: are they related?

Denis-Didier Rousseau et al.

Correspondence to: Denis-Didier Rousseau (denis-didier.rousseau@umontpellier.fr)

Supplementary material

Fig. S1. Detection of the major transitions in U1308 benthic $\delta^{18}O$ record (Hodell and Channell, 2016) using the KS augmented test by Bagniewski et al. (2021). The identified transitions correspond to the various boundaries between the marine isotope stages (MIS) determined during the past 3.2 Myr. In blue cooling transitions and in red warming transitions. The MIS labels are according to Lisiecki & Raymo (2005) while substage numbering is from Railsback et al. (2015).

Fig. S2. Detection of abrupt transitions in the NGRIP $\delta^{18}O$ record (Rasmussen et al., 2014)using the KS augmented test by Bagniewski et al. (2021).. In dark gray, Greenland interstadials, labeled for example GI-3, or Greenland interstadial "warm" substages labeled for example GI-8c. Greenland interstadial "cold" substages are in light gray. Events labeled in green or the greenbox indicate a disagreement between Rasmussen et al. (2014) interpretation and the KS test results. The red question marks are event not labeled in Rasmussen et al. (2014)

Fig. S3. Scatter plots a) of the DO duration (in yr b2k) versus the DO number; b) of DO relative sea-level variation (in m) versus DO duration (in yr b2k). The DO relative sea-level values are estimated from Waelbroeck et al. (2002) for the DO boundaries given by Rasmussen et al. (2014)

Table S1. Duration of the DO cycles as estimated from the NGRIP $\delta^{18}O$ boundaries from Rasmussen et al. (2014)

References

Bagniewski, W., Ghil, M., and Rousseau, D. D.: Automatic detection of abrupt transitions in paleoclimate records, Chaos, 31, 113129, https://doi.org/10.1063/5.0062543, 2021.

Hodell, D. A. and Channell, J. E. T.: Mode transitions in Northern Hemisphere glaciation: co-evolution of millennial and orbital variability in Quaternary climate, Clim. Past, 12, 1805–1828, https://doi.org/10.5194/cp-12-1805-2016, 2016.

Lisiecki, L. E. and Raymo, M. E.: A Pliocene-Pleistocene stack of 57 globally distributed benthic delta O-18 records, Paleoceanography, 20, PA1003, doi:10.1029/2004PA001071, 2005.

Railsback, L. B., Gibbard, P. L., Head, M. J., Voarintsoa, N. R. G., and Toucanne, S.: An optimized scheme of lettered marine isotope substages for the last 1.0 million years, and the climatostratigraphic nature of isotope stages and substages, Quat. Sci. Rev., 111, 94–106, https://doi.org/10.1016/j.quascirev.2015.01.012, 2015.

Rasmussen, S. O., Bigler, M., Blockley, S. P., Blunier, T., Buchardt, S. L., Clausen, H. B., Cvijanovic, I., Dahl-Jensen, D., Johnsen, S. J., Fischer, H., Gkinis, V., Guillevic, M., Hoek, W. Z., Lowe, J. J., Pedro, J. B., Popp, T., Seierstad, I. K., Steffensen, J. P., Svensson, A. M., Vallelonga, P., Vinther, B. M., Walker, M. J. C., Wheatley, J. J., and Winstrup, M.: A stratigraphic framework for abrupt climatic changes during the Last Glacial period based on three synchronized Greenland ice-core records: refining and extending the INTIMATE event stratigraphy, Quat. Sci. Rev., 106, 14–28, https://doi.org/10.1016/j.quascirev.2014.09.007, 2014.

Waelbroeck, C., Labeyrie, L., Michel, E., Duplessy, J. C., McManus, J. F., Lambeck, K., Balbon, E., and Labracherie, M.: Sea-level and deep water temperatures changes derived from benthic foraminifera isotopic records, Quat. Sci. Rev., 21, 295–305, 2002.

Detection of Abrupt transitions from benthic $\delta^{18}O$ in U1308 with the K-S method

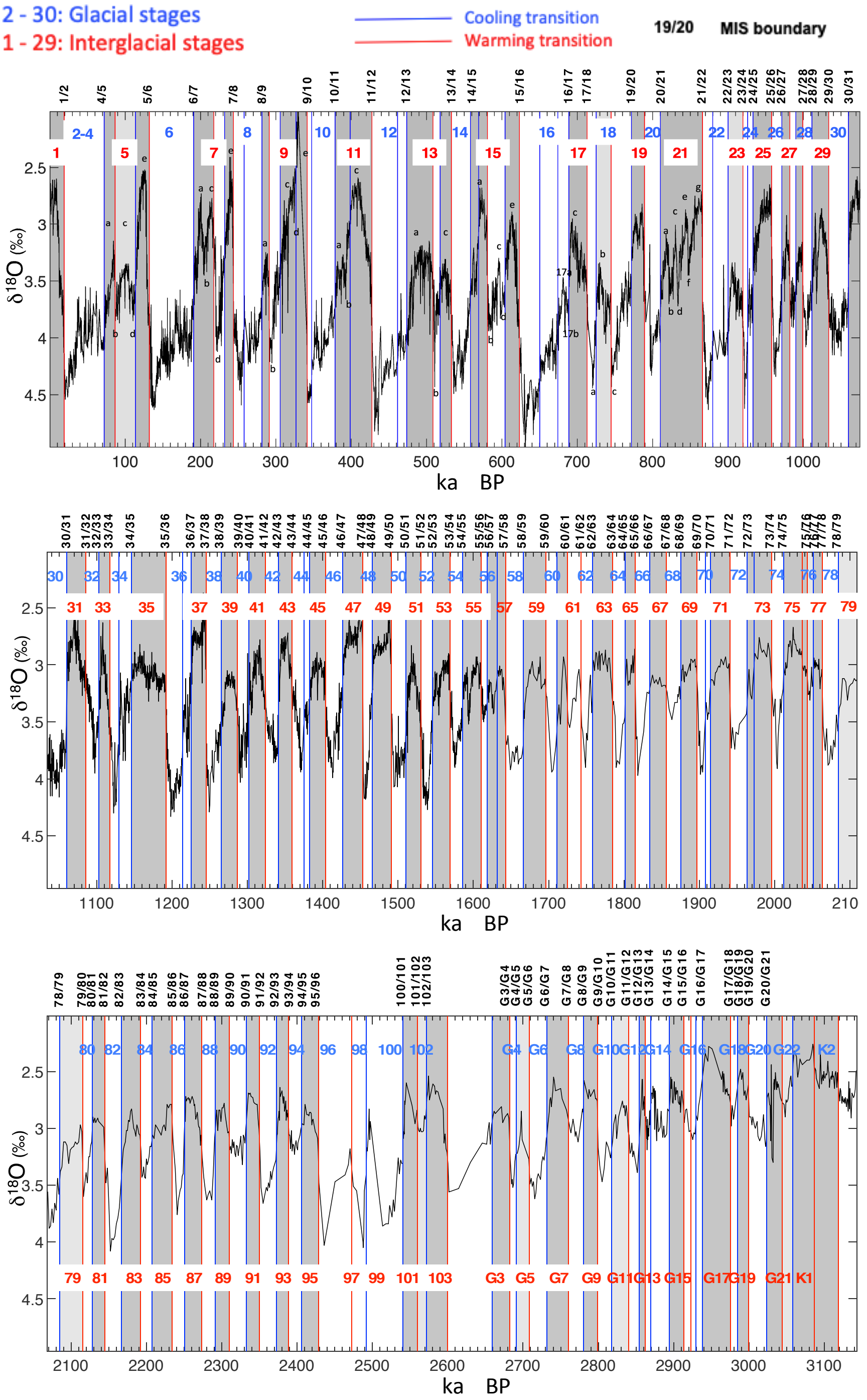

MIS boundaries from Lisiecki & Raymo (2005). Paleoceanography, PA1003, doi:10.1029/2004PA001071 and odd MIS from Hodell and Channel (2016) Climate of the Past, 12, https://doi.org/10.5194/cp-12-1805-2016.
Substage numbering from Railsback et al. (2015). Quaternary Science Reviews 111. https://doi.org/10.1016/j.quascirev.2015.01.012.

Fig. S1

Detection of Abrupt transitions in NGRIP d180 with the K-S method

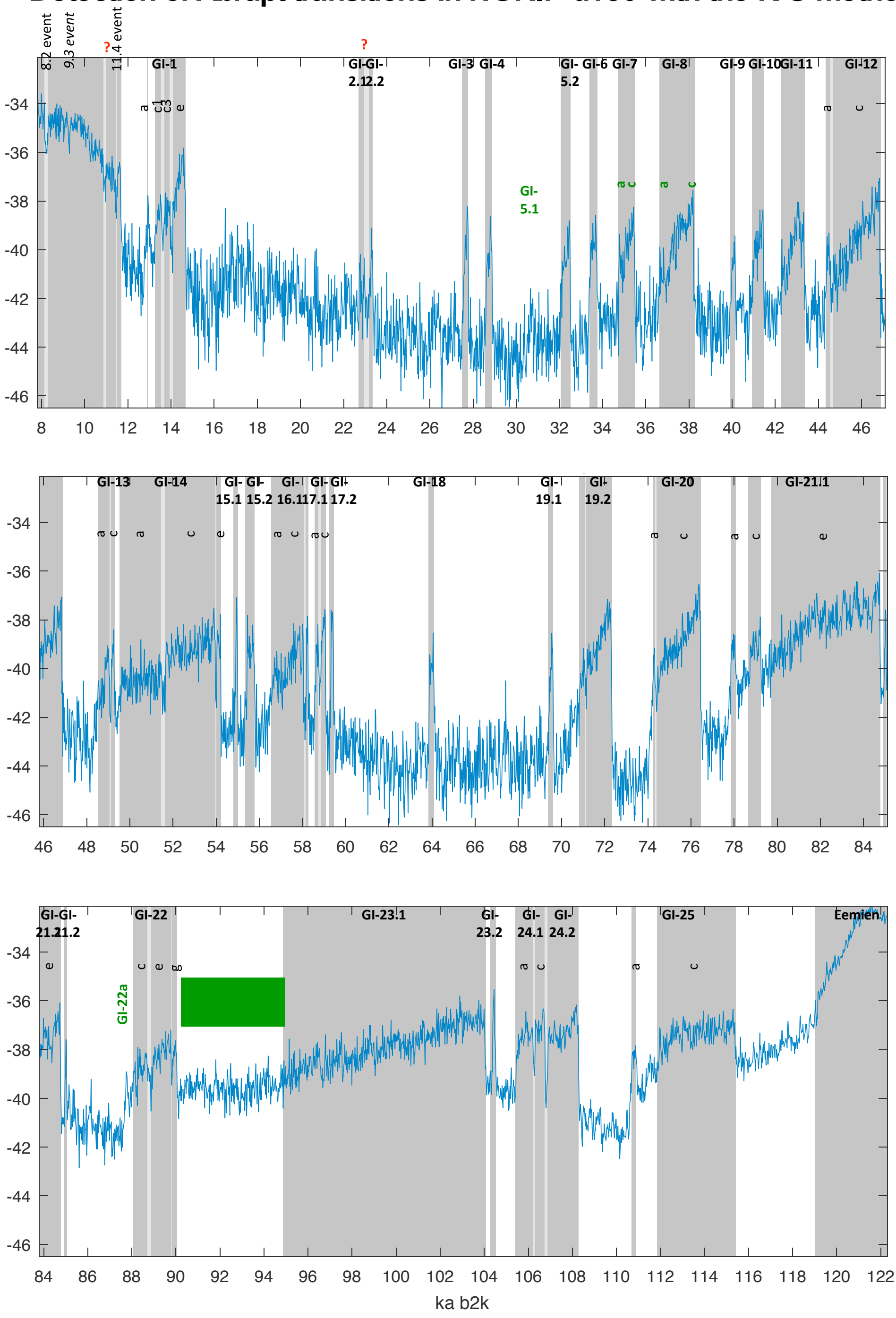

Fig. S2.

Scatter plots of the DO duration versus the DO number and the DO relative sea-level variation

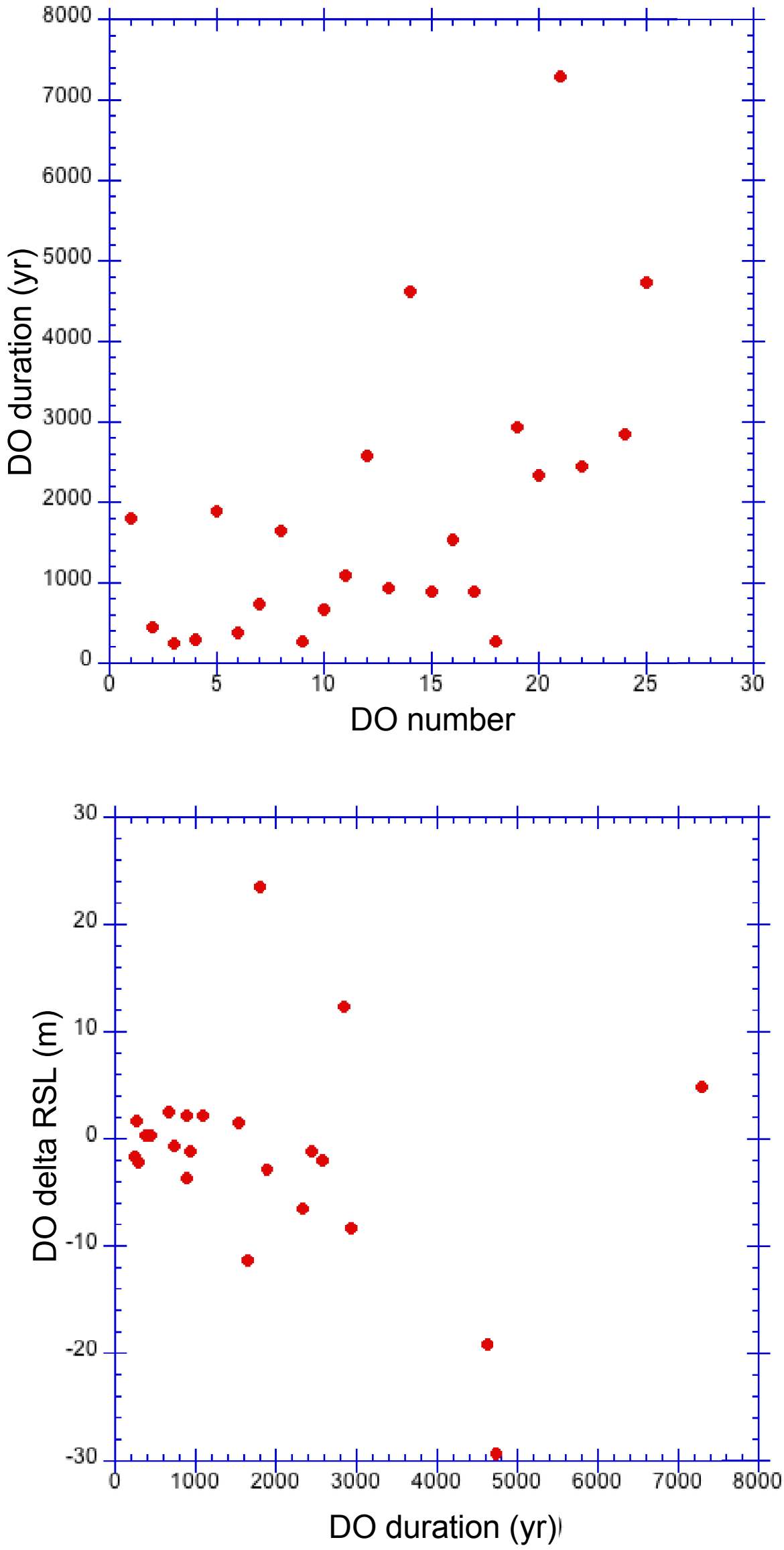

Fig. S3.

Table S1

Event	Age (yr b2k)	Duration DO cycle (in yr)	DO#	DO duration (in yr)
Start of Holocene	11703			
Start of GS-1	12896			
Start of GI-1a	13099			
Start of GI-1b	13311			
Start of GI-1c1	13600			
Start of GI-1c2	13660			
Start of GI-1c3	13954			
Start of GI-1d	14075			
Start of GI-1e	14692	2989	1	1796
Start of GS-2.1a	17480			
Start of GS-2.1b	20900			
Start of GS-2.1c	22900			
Start of GI-2.1	23020			
Start of GS-2.2	23220			
Start of GI-2.2	23340	8648	2	440
Start of GS-3	27540			
Start of GI-3	27780	4440	3	240
Start of GS-4	28600			
Start of GI-4	28900	1120	4	300
Start of GS-5.1	30600			
Start of GI-5.1	30840			
Start of GS-5.2	32040			
Start of GI-5.2	32500	3600	5	1900
Start of GS-6	33360			
Start of GI-6	33740	1240	6	380
Start of GS-7	34740			
Start of GI-7a	34880			
Start of GI-7b	35020			
Start of GI-7c	35480	1740	7	740
Start of GS-8	36580			
Start of GI-8a	36860			
Start of GI-8b	37120			
Start of GI-8c	38220	2740	8	1640
Start of GS-9	39900			
Start of GI-9	40160	1940	9	260
Start of GS-10	40800			
Start of GI-10	41460	1300	10	660
Start of GS-11	42240			
Start of GI-11	43340	1880	11	1100
Start of GS-12	44280			
Start of GI-12a	44560			
Start of GI-12b	44680			
Start of GI-12c	46860	3520	12	2580
Start of GS-13	48340			
Start of GI-13a	49060			
Start of GI-13b	49120			
Start of GI-13c	49280	2420	13	940
Start of GS-14	49600			
Start of GI-14a	51500			
Start of GI-14b	51660			
Start of GI-14c	53960			
Start of GI-14d	54020			
Start of GI-14e	54220	4940	14	4620

Start of GS-15.1	54900			
Start of GI-15.1	55000			
Start of GS-15.2	55400			
Start of GI-15.2	55800	1580	15	900
Start of GS-16.1	56500			
Start of GI-16.1a	57920			
Start of GI-16.1b	57960			
Start of GI-16.1c	58040	2240	16	1540
Start of GS-16.2	58160			
Start of GI-16.2	58280			
Start of GS-17.1	58560			
Start of GI-17.1a	58780			
Start of GI-17.1b	58840			
Start of GI-17.1c	59080			
Start of GS-17.2	59300			
Start of GI-17.2	59440	1400	17	880
Start of GS-18	63840			
Start of GI-18	64100	4660	18	260
Start of GS-19.1	69400			
Start of GI-19.1	69620			
Start of GS-19.2	70380			
Start of GI-19.2	72340	8240	19	2940
Start of GS-20	74100			
Start of GI-20a	74320			
Start of GI-20b	74440			
Start of GI-20c	76440	4100	20	2340
Start of GS-21.1	77760			
Start of GI-21.1a	78080			
Start of GI-21.1b	78740			
Start of GI-21.1c	79240			
Start of GI-21.1d	79700			
Start of GI-21.1e	84760			
Start of GS-21.2	84960			
Start of GI-21.2	85060	8620	21	7300
Start of GS-22	87600			
Start of GI-22a	87820			
Start of GI-22b	88000			
Start of GI-22c	88800			
Start of GI-22d	88920			
Start of GI-22e	89800			
Start of GI-22f	89840			
Start of GI-22g	90040	2440	22	2440
Start of GS-23.1	90140			
Start of GI-23.1	104040			
Start of GS-23.2	104380			
Start of GI-23.2	104520	14480	23	14380
Start of GS-24.1	105440			
Start of GI-24.1a	106220			
Start of GI-24.1b	106320			
Start of GI-24.1c	106750			
Start of GS-24.2	106900			
Start of GI-24.2	108280	3760	24	2840
Start of GS-25	110640			
Start of GI-25a	110940			
Start of GI-25b	111440			
Start of GI-25c	115370	7090	25	4730
Start of GS-26	119140			
	mean=	4045.08		

sd= 3178.87